

In Situ Thickness Measurements by
Laser Reflectance for Improved
MOCVD Process Development

Pratheep Balendra
and
Justin Daniel Meyer

Senior Design I

Advisor: Dr. Gallois
Dr. C. Dubourdieu

April 14, 1997

Abstract

In the development of a new MOCVD material there is a need for *in situ* monitoring of film growth. The design and implementation of a Laser Reflectance system will be discussed. Having integrated the Laser Reflectance system into the current MOCVD reactor, a few system refinements need to be made in order to increase signal clarity and to fix system anomalies. After the system is fully operational, the growth of Yttrium oxide was investigated. Experimental design and initial process parameter variation revealed rudimentary growth trends. Upon further investigation, parameter variation, and analysis of laser reflectance data, an optimal “operating window” for an unknown CVD material may be obtained in a development time comparable to other deposition techniques.

Outline

- Abstract
- Outline
- Introduction
 - Background
 - Problem
- Laser Reflectance
- Model
- System to Date
 - Reactor
 - Laser
 - Window
 - Substrate
 - Detector and power meter
 - Data Acquisition Card
 - Computer and DaqWare and Lab Windows/CVI
 - Overall System
 - Difficulties with LR
- Immediate Plans
 - Noise and Vibration
 - Window / Flange seals
 - Long Term Goals
- Data Analysis

- Summary
- Appendix
 - Appendix 1: Figures
 - Figure A
 - Figure B
 - Figure C
 - Figure D
 - Figure E
 - Figure F
 - Figure G
 - Figure H
 - Appendix 2: Film thickness
 - Appendix 3: Fresnel's equation
 - Appendix 4: Analysis Methods
- End-Notes

Introduction

The new growth in advanced electronics and optical devices has generated a need for single and multi-layered thin-film structures. These devices involve materials such as high temperature superconductors, ferroelectric, electrooptic, optical materials, diamonds, nitrides, semiconductors, insulators and metals in the form of ultra-thin layers at atomic dimensions.ⁱ Chemical Vapor Deposition (CVD) is widely used to manufacture these materials. Once the optimal operating window for the given material is known, the system may be automated and could run with minimal supervision. It would be reasonable to assume that every new assembly produced by the system would have the same properties.

Background:

When a new material is to be produced by CVD, the optimal growth conditions must be found. By employing the current methods, the process by which growth conditions and trends are observed is very time consuming and costly. Currently a substrate is placed in the reactor and a set of conditions such as heat and pressure are imposed upon the system. The system is allowed to come to a quasi-equilibrium under the imposed conditions. Then the precursors and reactants are flowed over the substrate. After a given period of time the substrate is cooled and removed to analyze for film growth. Then the process is started again with another set of conditions. It is estimated

that it would take about three or more hours for each cycle. Two runs a day is unacceptable.

Problem:

Film growth by Metal Organic Chemical Vapor Deposition (MOCVD) has traditionally lacked *in situ* growth monitoring. Processes such as Molecular Beam Epitaxy (MBE) have enjoyed the strength of *in situ* analysis tools, while MOCVD is at a disadvantage. Most tools employed by MBE, such as Auger and x-ray diffraction, require high or ultra-high vacuum conditions which are not applicable in MOCVD.ⁱⁱ Optical techniques seem a viable option.

There are three methods under consideration: Fourier Transformation Infrared spectroscopy (FTIR), Tunable Diode Laser Absorption Spectroscopy (TDLAS) and Laser Reflectance (LR). FTIR can be used to analyze the reaction products or exhaust gas. Since the initial gas composition is known, by analyzing the reaction products, film growth can be extrapolated.

TDLAS is a process that is currently being developed by Dr. Dubourdieu. In this process, an infrared diode laser is used to analyze the chemical composition of the gas directly above the substrate. By knowing the dynamics of the gas composition, film growth can be determined.

Laser Reflectance

The thickness of a thin film is measurable using laser interferometry. Similar methods are used in techniques such as ellipsometry, where the phase angle is varied and the changes in the intensity of the reflected beam is analyzed.

During Laser Reflectance as shown in Figure 1, a linearly polarized laser is impinging on the substrate. When there is no film, the P (parallel) component of the beam is totally transmitted and absorbed by the substrate at the Brewster angle. The S (perpendicular) component is almost, 65% at Brewster angle in silicon, reflected.

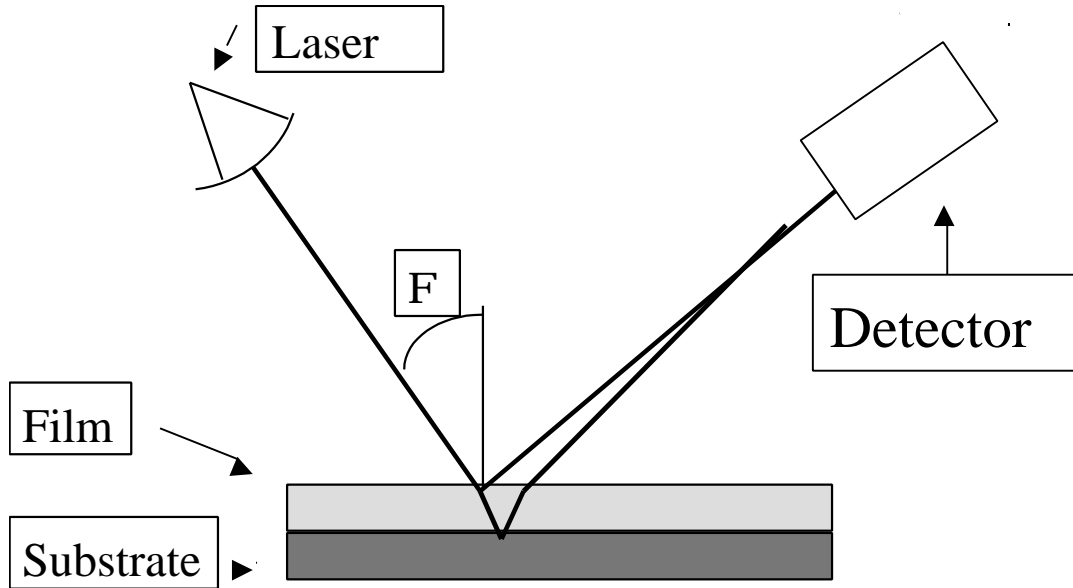


Figure 1.

The reflected beam is separated into S and P components. Each of the component beam is collected by a photodiode detector and the intensity is measured by power-meters. When a film begins to grow, there are two paths the beam follows. (refer to Figure 1) The first is the beam reflected off the surface of the film itself. This beam has both an S and a P component. The second path followed is the refraction path, where the light refracts into the film, is reflected off of the substrate, and refracted back out of the film, at a path parallel to the first. The phase difference between the paths may be equated to the

film thickness taking into account the dielectric function of the film and the angle of incidence.

Since the wavelength of the laser is fixed, and the thickness is increasing, there will be a cyclic effect to the intensity of the S and P components. The path difference, as it increases, will alternately become destructive and constructive. The periodicity of wave form is described by equation 1. (Refer to Appendix 2)

$$T = 1 / [2 * \text{SQRT}(n^2 - \sin^2 F)] \quad (1)$$

Unlike ellipsometry, where one needs to determine the order of the thickness by other methods, we can see the number of oscillations completed, if any, to determine true thickness.

Model

The interference model is based on Fresnel's equations. (Appendix 3) In the model, it is assumed that the extinction coefficient is zero and that the laser is impinged at Brewster's angle (75.6° for Silicon) at all times. Since the light is incident at Brewster's angle, plus or minus a couple of degrees, the P component is totally transmitted into the substrate, eliminating it from consideration at this point. The resulting interference curve is shown in figure 2.

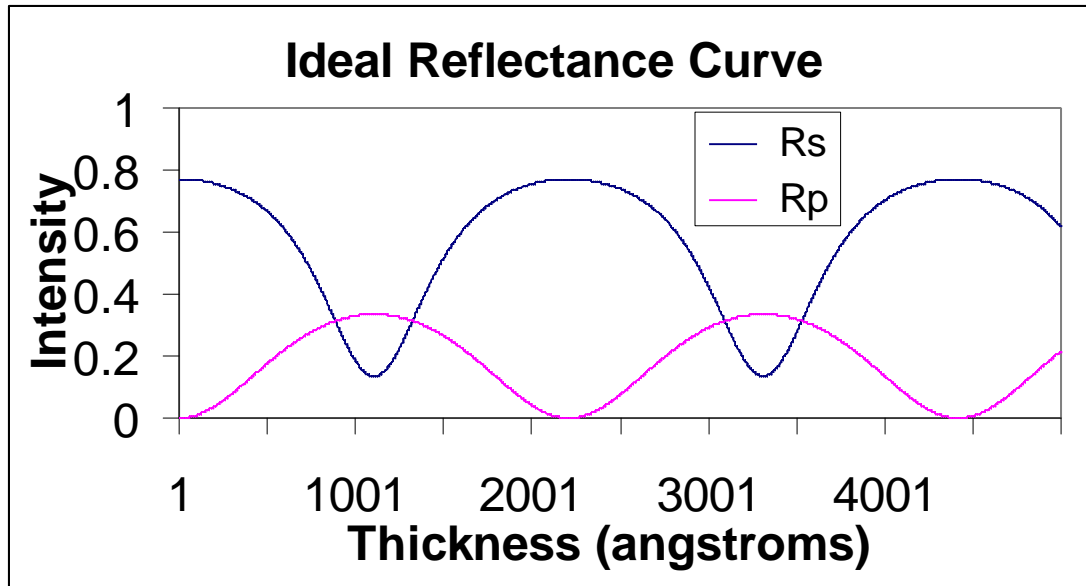


Figure 2.

The ideal interference curve from the model will assist us in accounting for several factors and phenomena in the course of the project. Firstly, the model will allow us to account for the effects of absorption, or signal attenuation. The model will also assist in monitoring the changes in the index of refraction (n) of the substrate, as n is dependent upon the temperature of the material. Nucleation of the thin films can not be modeled by the growth model.

System to-Date

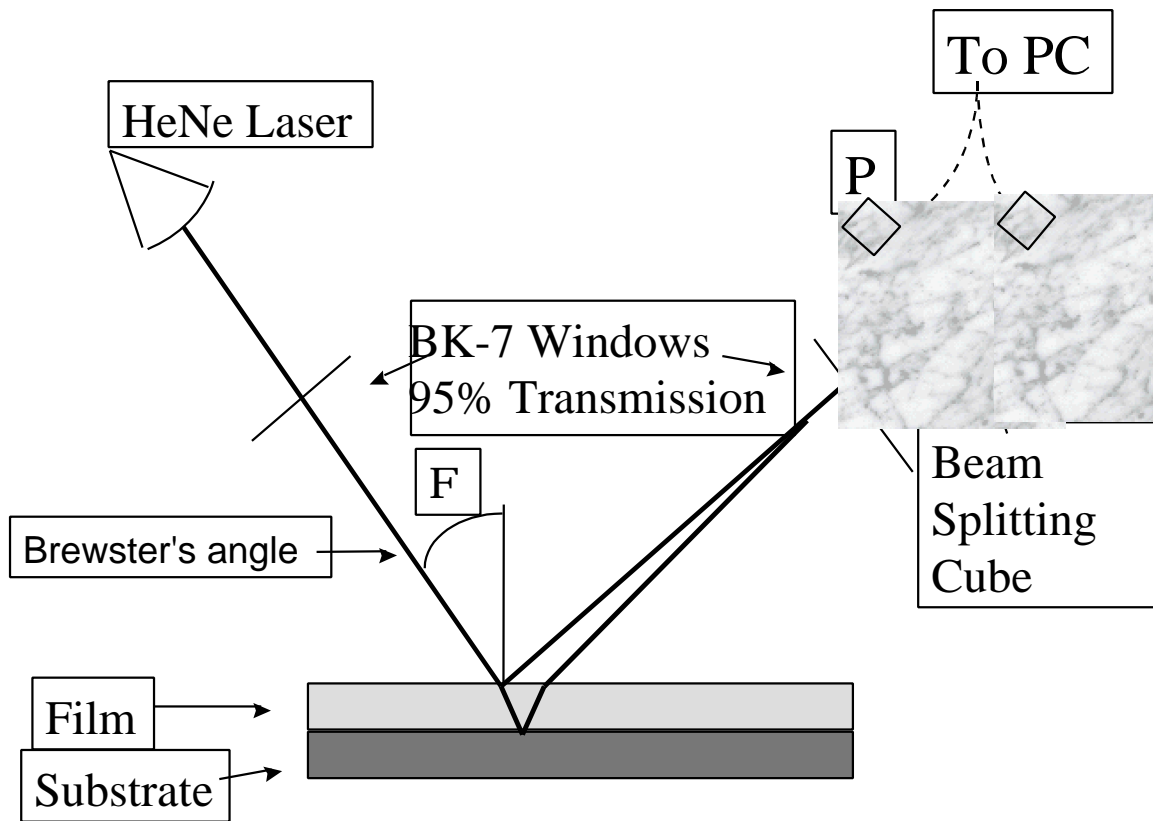


Figure 3.

Reactor:

The first portion of the system to be designed was the MOCVD reaction chamber. It is 12 inches tall by 8 inches in diameter made of stainless steel. 6.49 inches from the top is a horizontal opening with a radius of 0.69 inches. This port will be used for the IR spectroscopy. The port to be used for Laser Reflectance is 0.94 inches below and perpendicular to the center of the first port with a diameter of 1.87 inches.

The substrate will be held by the substrate holder/heater at 6.90 inches from the top of the chamber. It was designed so that the substrate will be visible parallel to the

center of the IR spectroscopy port. This is due to the fact that the IR laser beam must be able to enter the chamber and travel parallel close to the substrate and exit the chamber.

It was also intentionally designed so that the substrate will be above the Laser Reflectance port. This was done to facilitate the fact the laser light must be directed onto the substrate near the Brewster's angle, ranging from 60° to 80° , so that the reflected beam can escape the reaction chamber through the port and be analyzed. See Appendix 4.

Laser:

The laser that is being used is a Class IIIb (~ 8 mW) linearly polarized HeNe laser with a wavelength of 632.8 nanometers. This laser was used in the reflectance system because it had already been purchased. Other lasers were considered as candidates; yellow HeNe at 594.1 nm, green HeNe at 543.5 nm, blue HeCd at 441.6 nm and an ultra-violet HeCd at 325 nm. Shorter wavelengths provide better resolution.ⁱⁱⁱ In general applications the laser will be restricted to wave lengths that are transparent to the medium being studied.

Window:

It is desired that the optical windows be highly transmittable as not to absorb any light and reduce the intensity of the signal. It is also desired that the windows be flat and smooth so as not to scatter the light and cause non ideal behavior of the signals.

Two materials were considered as a suitable optical windows. The first was quartz glass. This would have a 95% transmittance and be relatively rough. The other choice was optical glass (BK-7). The transmittance of the optical glass is 95% and it may be polished optically smooth to eliminate the effects of scattering due to surface topology and defects. The glass was chosen as the window material since its properties were very

close to that of quartz and yet is was inexpensive in comparison to other optically flat windows.

Substrate:

When a film is grown, it will tend to mimic its growth medium. For example, if the substrate is stepped then the new film will also be stepped. In Laser Reflectance, it is desired for the film and the substrate to be smooth or flat. The flatter the surface the less scattering that will be caused by the light that is reflected off or transmitted through.

Silicon is chosen as the substrate, because it is widely used, can be polished to an exceptionally smooth finish, and its properties are well understood and its interaction with many films are already known. Silicon substrates are easily and inexpensively obtained. They can be made or bought very smooth and flat.

Detectors & Power Meters:

The detectors are two Newport low-power detectors, model 818-SL. The photodiode detectors, along with the power meters to which they are connected, were supplied by Dr. Gallois. The detectors output a voltage which is read and displayed by the power meters and channeled to an analog output for signal acquisition and analysis. The power meters measure the power from the photodiodes. Integrated into the meters are zeroing dials to account for ambient light and environmental conditions (such as temperature) which affect the operation of the photo diodes. The meters also have 6-orders-of-magnitude amplification circuitry, to ensure that the output signal is detectable. The analog output voltage ranges between 0 and 2 volts.

Data Acquisition Card:

For data acquisition, we determined we would need at least 2 analog (finely graded: around 2^{10} gradations) input channels, one each for the S and P components of the reflected beams. Since process control was a likely in the future, at least 2 analog outputs were necessary. Digital (high/low) channels were also a plus, possibly for valve control.

With the assistance of parameter selection software by National Instruments (NI) and guidance by Dr. Gallois, the “Lab-PC+” data acquisition (DAQ) card was selected and purchased. The DAQ card is an XT bus card with 4 differential input channels, 2^{12} resolution, 83.3 kB/s sample rate across all channels, and a 10 volt input range. The two analog output channels have the same resolution and range. This particular card also features 24 digital output channels and 3 timers.

To interface with the card, a connecting ribbon cable and terminal block were also purchased from NI. From the terminal block, wires were connected to a lab-constructed BNC (co-axial) terminal box. Two BNC cables connected the terminal box to the power meters. The introduction of standard, modular interfaces will aid in future uses and adaptations to other systems.

Computer & DAQ Views:

The DAQ card was installed in a computer purchased by Dr. Gallois for the experiment. The Pentium 90 system has 32 MB of memory and a more than ample amount of disk space for storing data files. Currently installed on the system is DAQ View, NI’s own data acquisition software, shipped free with every DAQ card purchased.

Once the signal is digitized and given to the computer, it is easy to analyze. This software, DAQViews, is able to detect the card in the computer and then display the information being received by the card as a graph or in a tabular form. The tabular data can be imported into a spreadsheet, assembled with the model to produce the thickness of the film as it grows.

We have performed basic data acquisition and viewing using this software, although we will almost definitely be moving up to a more powerful program-LabWindows/CVI, a copy of which is owned by Dr. Gallois. Recently we have moved away from DaqWare, a primitive software and started using LabView, Student Edition. This interface is capable of real-time display as well as some post processing of data.

In the future, this computer will be integrated with the IR spectroscopy being done by Dr. Dubourdieu. There is also the distinct possibility of Fourier Transform IR spectroscopy being used to analyze the reaction products. Once all of these systems are fully refined, they will be integrated on this one computer.

Overall System:

A pictorial view of the overall system is in figure 5, below. As can be seen, the laser is reflected off the substrate in the reactor, whereupon is 'caught' by the detectors.

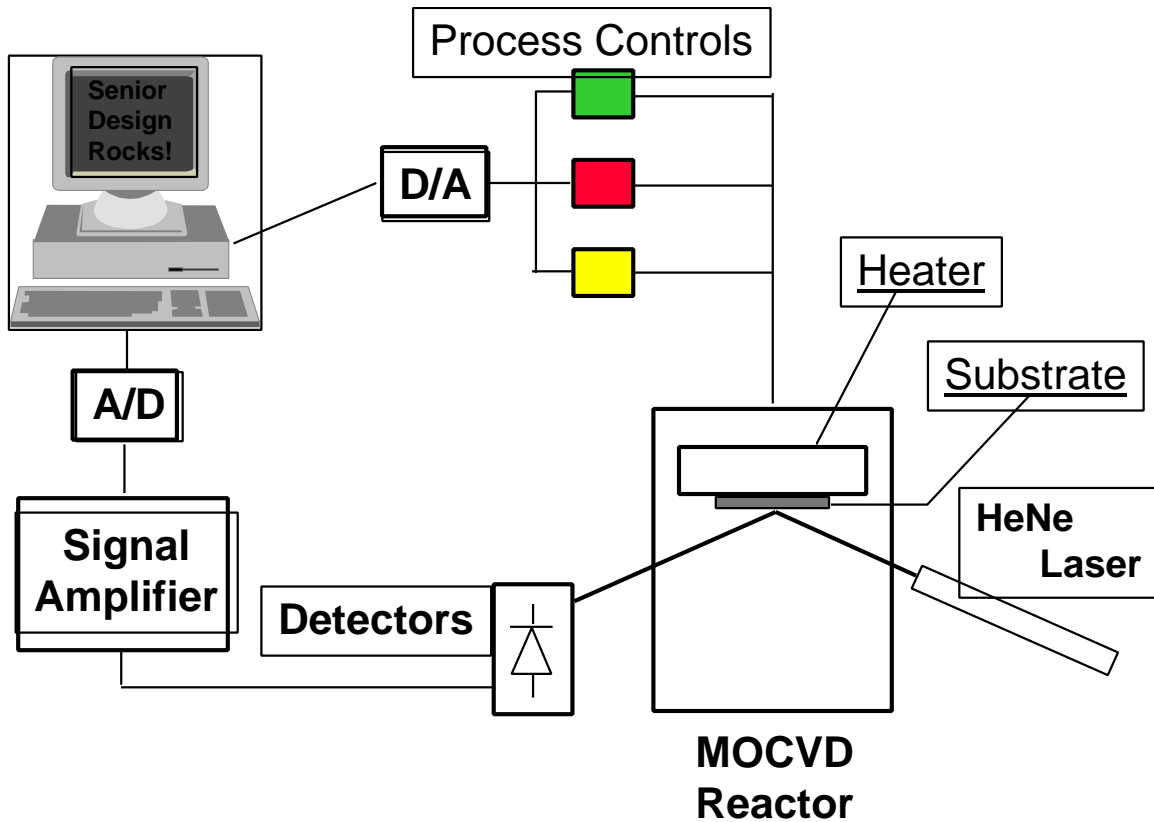


Figure 4.

The signal intensity is measured by the power meters and recorded by the DAQ card which processes the signal with a A/D converter. Through a graphical interface, the computer displays and stores the signal information as it processes it. Using a process control algorithm, process parameters can be varied by the computer and the effects measured by the system over a defined period of time before the cycle continues.

The purpose of this project is to shorten the development time of MOCVD materials. With the setup depicted in figure 4, this can be achieved. First, the operator chooses which process parameters to vary in the algorithm software. Conducting ½ hour runs under each scenario, 192 combinations could feasibly be completed, including setup

time and trend analysis. At the present, only 10 runs can be achieved within a typical work week. Analysis of growth trends in the experiment results cell will determine an operating window and/or the need to refine the varied parameters and repeat the process.

Difficulties with LR:

Vibration is a culprit of signal degradation. Mechanical vibration due to moving parts of the MOCVD system affect the position of the substrate with respect to the laser. This results in loss of signal accuracy.

Another culprit which can produce effects similar to that of mechanical vibration is electrical noise. Electrical noise is the result of fields surrounding power supplies, wires, in fact all electrical equipment- and especially computer components. Electrical noise typically can be reduced significantly reduced with increased shielding, but one can not shield everywhere, such as inside the computer cabinet. The noise attributable to vibration and the remaining electrical fields must be filtered or accounted for in data acquisition. A major component was the laser power supply. Despite shielding it affected DAQ and was, in the end, moved 5 feet away. We will use signal processing in LabWindows/CVI to attempt to account for some noise created by these and other causes.

One other problem that was encountered with CVD of THF-soluble precursors is that the THF solvent in the liquid precursor dissolved in the vacuum pump oil and increased its vapor pressure. The oil vapor diffused its way against the vacuum and re-condensed on cooler part of the system- O-rings, clamps, and edges. This forced us to abandon the liquid source and move to solid source. The pump oil was changed and the pump became noticeably more efficient. As the problem only evolved of late, it

would appear that the THF content in the pump oil built up over a period of about six months. To return to liquid source and thus THF-soluble precursors, a different solvent must be used, the pump oil changed every four months (or as necessary), or the use of a special oil implemented. One of the first to may be justifiable by the ease of use and consistency of precursor delivery which the use of liquid precursors affords one.

Further Improvements

Noise & Vibration:

Now that the system is integrated to the MOCVD reactor and has been in use for a while, there are some refinements that need to be made. These refinements will increase signal clarity and allow for optimal performance. From the test run it can be seen that there is some electrical noise. The source of the anomalies are not well known. There still seems to be some common grounding issues that are the cause of some noise. The operation manual for the Data Acquisition card gave an example of a hardware filter that needs further investigation.

Using the suggestions from NI we implemented the filter circuit as show in figure 5. This filter was able to reduce the noise to the limits of the DAQ card. One draw back to this circuit was that it reduced the value that was being read by the bower meter by about 0.5 volt. Due to some time constraints this filter was not evaluated further and implemented. The noise was dealt with by averaging about a select number of data points (usually about 80 points) together and making it one data point.

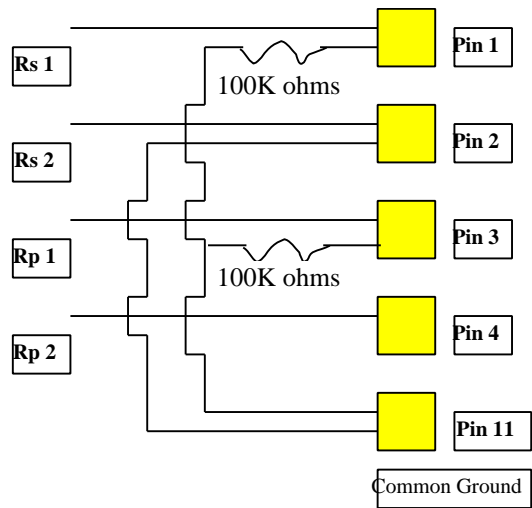


Figure 5

During the dry runs it was found that the signal would fluctuate when there was no theoretical reason. By dampening vibration to the MOCVD chamber and the Laser Reflectance system the non ideal behavior was reduced. One method to dampen the vibration is to design a better chamber mount. The current mount is a composed of two sheets of aluminum that are sitting on three posts attached to the optical bench. The chamber is screw clamped onto the aluminum sheets. Since the sheets are flexible and the clamps have no proper place too attach, the chamber vibrates. By designing a mount that is fixed rigidly to the optical table and can repeatedly hold the chamber in the same place would help reduce some of the mechanical vibration and help in the alignment of the laser relative to the substrate.

Different holder mechanisms were examined and it was determined that to make a holder that had adjustable legs and still remain stiff would not be a simple stand

but be a large framework for the entire chamber. It was recommended that the ¼ inch aluminum sheet be replaced with a ½ inch or more thick aluminum plate. That would stiffen the base where the chamber is attached and possibly reduce the vibration. This is yet to be implemented.

Window/Flange Seals:

In the beginning, the optical windows were held vacuum tight by a quick-and-dirty method. High vacuum grease is used to hold the windows to the flanges. The grease also functions as vacuum seal with proper monitoring. At higher temperatures the grease is not effective. It loses its viscosity and starts to flow more rapidly into the system. The grease becomes a source of contamination and the windows become a source of pressure leak. We place rubber O-rings between the optical window and the port flange to produce a vacuum seal. This worked well but the conventional flange clamps produced enough stress on the glass windows to break them. A window holder was designed and implemented this semester. It has held a good vacuum and does not stress the window to the point of failure.

Long-term Goals

The goals for future are first to accurately and reproducibly determine the exact thickness of the film at question. This will be attained through above mentioned system refinements.

The current method does not allow for the operator to view the thickness of the film in real time. This will be addressed by employing LabWindows/CVI. This software will perform two functions. First it will replace DAQViews in controlling and obtaining information from the card. LabWindows/CVI will also have the ability to incorporate the

model to facilitate real-time film thickness analysis. The programming could also be modified to have a process control algorithm that would automatically control various parameters based on calculated film growth. This would lead to the desired and complete system that can be automated so that an operating window for a new material can be found in a relatively short amount of time.

Data Evaluation

In between system modifications and fixes, twenty-three samples (over 30 runs) were conducted. More than half of the experiments were inconclusive due to lack of data acquisition. Appendix 1 contains the reflectance results from eight 'successful' samples. In all cases, even when not marked, the p (parallel) component is the dark trace and the s (perpendicular) component is the lighter of the two and should be 90° out of phase at all times. And, except where noted, all films grown are Yttrium Oxide (Y_2O_3) on silicon.

While system pressure and source infusion rates were varied, all other conditions were held close to nominal values. Due to the time required for the system to reach equilibrium after any changes are made, they were rarely varied. The substrate temperature was held as near to 800°C as possible, with some drift over time due to increasing inefficiency- resulting in a final substrate temperature of 475 to 600°C. System lines were held between 250 and 300°C. The solid source was run at 325°C and the liquid source at 200°C.

Figure A is a composite figure of three runs on one sample. The traces are discontinuous due to changes in laser and detector alignment. The source is 0.05 molar THF (with 10% tetraglyme) fed at a rate of 0.75 ml/min in the first region and 0.9 ml/min

in the latter two. Film growth in each of the three regions is 342 angstroms/min (A/min), 346 A/min, and 352 A/min, respectively- despite the different infusion rates. This would be indicative of a maximum growth rate under those conditions. Some of the periodic inconsistency may be attributed to the large number of air bubbles which were introduced at the check-valve.

Figure B is comprised of four 'zones' with a different ambient pressure in each. The pressures for each of the regions are 3 torr (up to time marker 5050), 10 torr (5050 to 10075), 6 torr (10075 to 15050), and 3 torr (15050 to 20000). The remaining time is an attempt at a pressure of 1 torr, but the system could not maintain a pressure less than 2 torr. The growth rates achieved were 210 A/min, 204A/min, 160 A/min, and 11.4 A/min, respectively. This indicates a potential general upward trend in growth with respect to system pressure, but is not decisive, due to the downward, unknown trend across regions.

Figure C is a reflectance curve of Lithium Niobate (LiNbO_3). Over a period of nearly two hours, a film of nearly 11,000 Angstroms was grown. This was the only really good data acquired for lithium niobate deposition. Yttrium oxide on silicon is again the subject in Figure D. Despite the asymmetrical attenuation, a growth rate of about 150 A/min was achieved at an ambient pressure of 3 torr.

In Figure E, the carrier gas flow rate was changed from 200 sccm to 800 sccm, resulting in a drop in the growth rate- from 350 A/min to 150 A/min. Figure F is one of the cleanest curves obtained. A sample average rate of 100 was used to eliminate residual noise. The s component is actually two orders of magnitude less than the p component. The p component also exhibit very characteristic attenuation due to absorption of the light by the yttrium oxide. A growth rate of 37 A/min was achieved on this silicon sample.

Figure G is a five minute run conducted with the aim of investigating the film nucleation mechanism. The data was averaged at a ratio of 80 samples to 1 point, providing a commensurately high signal-to-noise ratio.

In the solid source run conducted on sample 23, the packing density of the powder was varied. The first centimeter was 1.6 g/cm, and the second was about 0.8 g/cm. A drastic change in the growth rate is evident, although more data needs to be collected before any assertion is more than just unsubstantiated speculation.

The beginnings of several trends were evident in the process of data evaluation. System conditions conducive to yttrium oxide film growth on silicon include: relatively low carrier gas volume, on a scale of 200 to 800 sccm; and high ambient pressures, over 3 to 10 torr. These are only two trends at a set of system temperatures. An operating window would resolve when temperature were varied as well as pressure and flow rates.

Summary

Over the course of the past semester, a Laser Reflectance system was successfully designed to measure film thickness in real-time. With the implementation of system refinements to increase signal clarity and other improvements, the system was brought into full, almost nearly unassisted operation. Human intervention, however, is still necessary to interpret the reflectance data for optimal interpretation. In the near future, through process parameter variation, a growth database will be created on a new material. From this information, an operating window for the MOCVD material will be apparent.

Appendix 1

Appendix 3

$$\text{Ang} := 10^{-10} \quad \phi_B := 74.5 \text{ deg} \quad \epsilon_a := 1 \quad \epsilon_f := 1.8 \quad \epsilon_s := 15.25$$

$$\text{nm} := 10^{-9} \quad \lambda := 632.8 \text{ nm} \quad \phi_0 := \phi_B \quad i := \sqrt{-1} \quad d_f := 0, .2.. 50$$

$$r_{\text{afp}} := \frac{\epsilon_f \cos(\phi_0) - \sqrt{\epsilon_a} \cdot \sqrt{\epsilon_f - \epsilon_a \cdot \sin(\phi_0)^2}}{\epsilon_f \cos(\phi_0) + \sqrt{\epsilon_a} \cdot \sqrt{\epsilon_f - \epsilon_a \cdot \sin(\phi_0)^2}} \quad r_{\text{fsp}} := \frac{\epsilon_s \cdot \sqrt{\epsilon_f - \epsilon_a \cdot \sin(\phi_0)^2} - \epsilon_f \sqrt{\epsilon_s - \epsilon_a \cdot \sin(\phi_0)^2}}{\epsilon_s \cdot \sqrt{\epsilon_f - \epsilon_a \cdot \sin(\phi_0)^2} + \epsilon_f \sqrt{\epsilon_s - \epsilon_a \cdot \sin(\phi_0)^2}}$$

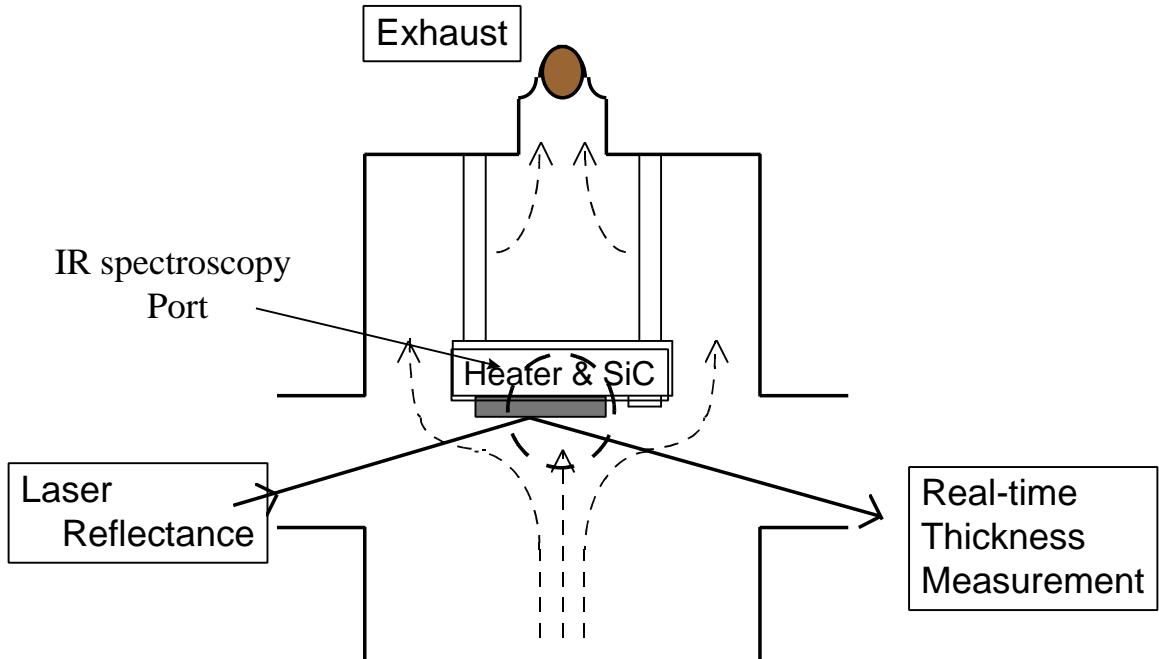
$$\Phi(d_f) := \frac{2 \cdot \pi \cdot d_f}{\lambda} \cdot \sqrt{\epsilon_f - \epsilon_a \cdot \sin(\phi_0)^2}$$

$$r_{\text{p}}(d_f) := \frac{r_{\text{afp}} + r_{\text{fsp}} \cdot e^{-2 \cdot i \cdot \Phi(d_f)}}{1 + r_{\text{afp}} \cdot r_{\text{fsp}} \cdot e^{-2 \cdot i \cdot \Phi(d_f)}} \quad r_{\text{conj}}(d_f) := \frac{r_{\text{afp}} + r_{\text{fsp}} \cdot e^{2 \cdot i \cdot \Phi(d_f)}}{1 + r_{\text{afp}} \cdot r_{\text{fsp}} \cdot e^{2 \cdot i \cdot \Phi(d_f)}}$$

$$R(d_f) := \sqrt{r_{\text{p}}(d_f) \cdot r_{\text{conj}}(d_f)}$$

$$T(d_f) := R(d_f) \cdot \Phi(d_f)$$

Appendix 4



ⁱ Auciello, Orlando and Krauss, Alan R. *Why In Situ, Real-Time Characterization of Thin-Film Growth Processes?* MRS Bulletin, May: 1995.

ⁱⁱ Bajaj, J., et al. *Modeling of In Situ Monitored Laser Reflectance During MOCVD Growth of HgCdTe* Journal of Electronic Materials. Vol. 22, Nov: 1993. Page 899

ⁱⁱⁱ Saenger, K. L. and Tong, H. M. *Laser Interferometry: A Measurement Tool for Thin Film Polymer Properties and Processing Characteristics*. IBM Research Report. Yorktown Heights, NY: RC 14238 (#63452) 11/8/88.